Check for updates

Evaluation of Indian Summer Monsoon Rainfall Using the NCEP Global Model: An SST Impact Study

ANCY THOMAS[1]

Abstract—The study evaluates the Indian summer monsoon prediction skill of the Atmospheric General Circulation Model (AGCM) and the impact of sea surface temperature (SST) boundary forcing on the model performance. The National Center for Environmental Prediction's (NCEP's) T170/L42 AGCM model configured with a horizontal resolution of 75×75 km, with 42 vertical levels is used for the study. The SST-rainfall relationship is examined in the coupled Climate Forecast System version 2 (CFSv2) model, as CFSv2-predicted SST is used as input for the T170 model. The NCEP Global Forecast System-T170 (GFS-T170) simulations are carried out with boundary forcing of observed SST, CFSv2-predicted SST and the bias-corrected CFSv2 SST. An ensemble of seasonal runs was made using the initial conditions of May to September, and integrated up to September 30th. The significance of discontinuity in the initial conditions due to climate forecast system reanalysis (CFSR) is assessed based on the two-period approach of climatology for the two time scales of 1985–1998 and 1998–2009. CFSv2 predicted climatological summer monsoon rainfall with a significant dry bias over the three convection zones; Western Ghats, Central India and North-east India, and cold bias over the Indian ocean basin and central equatorial Pacific, with strong cold bias over a narrow region of equatorial Pacific. The model could capture 64% (16 out of 25) of the year's rainfall anomaly signal. The skill of the model is improved in the recent period (1999–2009). The model could simulate the negative Nino 3 and excess rainfall and the La Nina event realistically for the year 1988. The model shows a large difference in Nino indices for the years 1987 and 1998, which led to the unrealistic rainfall simulation. The model has a low skill for indicating the relationship between the Indian Ocean Dipole (IOD) and Indian summer monsoon rainfall (ISMR). The CFSv2 model could not capture the strong positive correlation of the IOD and strong negative correlation of Nino 3 with the ISMR for the period 1999–2009 realistically, suggesting improvement of SST simulation in the CFSv2 model. The T170 model forced with observed SST shows wet bias in peninsular India and dry bias over Northeast India, whereas that of CFSv2-predicted SST simulated a wet bias in peninsular India and widespread dry bias in North and Central India. When the model was forced with bias-corrected CFSv2 SST, the dry bias improved in North and Central India, and the intensity of wet bias increased in peninsular India. The model could capture 56, 48 and 64% of the year's rainfall anomaly signal (positive or negative) correctly in the same sign for being forced with observed SST, CFSv2-predicted SST, and bias-corrected CFSv2 SST, respectively.

Key words: Indian summer monsoon rainfall, sea surface temperature, climatology, inter-annual variability.

1. Introduction

In a climate change scenario, prediction of ISMR has remained a challenge for atmospheric models (Wang et al. 2005; Gadgil et al. 2005). The study on both atmospheric and coupled atmosphere–ocean models revealed that there are difficulties in the representation of the mean Indian monsoon and its variation on different time scales (Gadgil and Sajini 1998; Kang et al. 2002; Wang et al. 2004; Rajeevan and Nanjundiah 2009). The slowly varying sea surface temperature (SST) boundary forcing plays a major role in the model's dynamical seasonal prediction skill of the Indian summer monsoon. It is noticed that the performance of the model depends on SST and rainfall correlation in Indian summer monsoon simulation (Wang et al. 2005; Kang and Shukla 2005). Models are generally inefficient at capturing realistic SST-rainfall relations (Bollasina and Nigam 2009; Rajeevan et al. 2012).

The EI Nino Southern Oscillation (ENSO) and Indian monsoon rainfall are known to have an inverse relationship, which has been observed in the rainfall spectrum exhibiting a spectral dip in 3–5-year period band. Spectral analysis of future climate projections by 20 Coupled Model Inter-Comparison Project 5 (CMIP5) models shows the possible shift in the ENSO-ISMR relationship under future global warming, and the

[1] Centre for Development of Advanced Computing, C-DAC Innovation Park, Panchvati, Pashan, Pune 411008, India. E-mail: ancymolt@cdac.in

study revealed that this spectral dip (3–5 years) is likely to shift to shorter periods (2.5–3 years) in the future (Azad and Rajeevan 2016). To deepen the understanding of the ISMR on decadal to multi-decadal timescales, ensemble simulations for the period AD 1600–2000 is carried out by the coupled Atmosphere–Ocean–Chemistry–Climate Model. Although the model largely underestimates the ISMR, it realistically reproduces the spatial patterns of its climatology and can further help in understanding the physical processes that govern the decadal to multi-decadal scale variability of the ISMR (Malik et al. 2017).

The performance evaluation of seven fully coupled model ensemble systems [DEvelopment of a European Multimodel Ensemble system for seasonal to inTERannual prediction (DEMETER) Multimodel Ensemble (MME)] in Indian summer monsoon simulation found that the MME performs better in simulating ENSO indices, but not in simulating ISMR and the Indian Ocean Dipole (IOD) (Preethi et al. 2010). They found that model skill of ISMR simulation for the earlier period of 1959–1979 is closer to the 'perfect model' score, but large differences are observed in the later period of 1980–2001, due to large biases in predicted SSTs over the Indian Ocean region and teleconnections between monsoon, ENSO, and IOD, indicating strong dependency of model-simulated Indian summer monsoon on initial conditions. Recently, there has been an improvement in the skill of ISMR prediction with coupled models (Rajeevan et al. 2011). The ENSEMBLE models are able to simulate/predict at least the sign of the ISMR anomaly in most of the extreme rainfall years; its performance in the drought years like 1972, 1974 and 1982 and the excess year of 1961 was particularly better than the DEMETER MME. However, the ENSEMBLE MME could not capture the recent weakening of the ENSO-Indian monsoon teleconnections, resulting in a decrease in the prediction skill compared to the 'perfect model' skill during the recent years, similar to DEMETER MME skill. Another ensemble prediction system using CFSv2 underestimates both the mean and variability of ISMR, whereas it simulates the northward propagation of monsoon intraseasonal oscillation reasonably well (Abhilash et al. 2013). These studies point out the importance in improving individual models for ISMR prediction.

There have been studies on the successful simulation of many of the features of the Asian/Indian summer monsoon by the National Center for Environmental Prediction (NCEP) Coupled Forecast System version 2 (CFSv2) (Pokhrel et al. 2013; B. Goswami et al. 2014; Hazra et al. 2015; Sahai et al. 2015). Pervasive cold SST bias in the CFS simulation in the context of moisture flux exchange between the atmosphere and the ocean shows that CFS simulation complies with the distinct feature of the observed mean annual cycle of evaporation and precipitation, but with the additive systematic bias over most of the region. Also, El Niño and the negative IOD seem to have much better control over the interannual variability of evaporation in the CFS simulation, contrary to the observation where El Niño and positive IOD have a larger say (Pokhrel et al. 2012). CFSv2 in simulating the Indian summer monsoon is evaluated in the context of the global monsoon in the Indo-Pacific domain and its variability. Although the CFSv2 captures the Indian summer monsoon spatial structure qualitatively, it demonstrates a severe dry bias over the Indian subcontinent. The leading mode of the June–September averaged CFSv2 rainfall anomalies covering the Indian summer monsoon and its adjacent oceanic regions are qualitatively similar to that of the observations, characterized by a spatial pattern of strong anomalies on either side of the Indian peninsula as well as the centre of opposite sign over Myanmar. However, the model fails to reproduce the northward expansion of rainfall anomalies from Myanmar, leading to opposite anomalies over northeast India and the Himalayas region (Shukla and Huang 2015). The possible reason of dry precipitation bias in CFSv2 during the Indian summer monsoon (June–September) and linkage between cloud physics, thermodynamics, and dynamics are identified; hence, the CFSv2 model improvement can be achieved by modification of the microphysical tendency equation for better representation of the vertical profile of cloud hydrometeors through improving the existing cloud microphysical parameterization (Hazra et al. 2016).

It is seen from the CFSv2 analysis on the simulations, with a default simplified Arakawa-Schubert (SAS) scheme and a revised SAS schemes, that the revised SAS scheme is able to reduce some of the

biases of CFSv2 as compared to the default SAS scheme. In a diurnal run with the revised SAS scheme, improvement of the diurnal cycle of total rainfall by improvement of the convection and associated convective rainfall has resolved a long-standing problem of dry bias by CFSv2 over the Indian landmass and wet bias over equatorial Indian Ocean, though the cold tropospheric temperature bias and low cloud fractions need further improvement (Ganai et al. 2015). The simulation and prediction skill of the Indian summer monsoon at two different horizontal resolutions viz., T126 (~ 100 km) and T382 (~ 38 km) using 28 years of hindcast runs of the CFSv2 model found that in the high-resolution run, the systematic bias in the teleconnection between the ISMR and IOD was considerably reduced (Ramu et al. 2016). These two versions of the CFSV2 model with two horizontal resolutions are used to study two different ENSOs, the canonical east Pacific type and the Modoki/central Pacific type (Pillai et al. 2017). They confirm that a higher-resolution CFSv2 is required to differentiate the flavours of ENSO and their teleconnections properly.

The performance of CFS over the Indian monsoon region in a 100-year coupled run stated that the biases of SST and rainfall affect both lower- and upper-level circulations in a feedback process, which in turn regulates the SST and rainfall biases by maintaining a coupled feedback process (Pattanaik and Kumar 2010). Simulation of the Indian summer monsoon and its intraseasonal oscillations in the CFSv2 model shows that there is possible bias in the co-evolution of convection and SST in CFSv2 over the equatorial Indian Ocean (Goswami et al. 2014). The skill of the CFSV2 model in seasonal prediction of ISMR at different lead times depicts the unrealistic teleconnection of ISMR with the IOD and unrealistic Equatorial Indian Ocean Oscillation, which suggests that the air–sea interaction in the Indian Ocean requires improvement (Chattopadhyay et al. 2016). The equatorial central Pacific SST and rainfall show very strong cold and dry biases, respectively, and these biases are due to strong unrealistic coupled feedback in this region. The prediction skill of the CFSv2 model in all ISMR basically comes from the ENSO-monsoon teleconnections and the inadequate representation of the Indian Ocean coupled dynamics

(George et al. 2016). The CFSv2 study on the role of monsoon intraseasonal oscillation and its interannual variability in simulation of seasonal mean rainfall shows that regardless of a reasonable ENSO-monsoon teleconnection in the model, the overestimated SST-convection relationship over the Arabian Sea hinders the large-scale influence of the ENSO over the Indian summer monsoon region and adjacent oceans (Pillai and Aher 2016). The study highlights that along with the successful simulation of intraseasonal oscillation, relationship with the boundary forces also needs to be captured well in coupled models for the accurate simulation of seasonal mean anomalies of the monsoon and its teleconnections.

The sensitivity to the initial conditions and model physics for ISMR simulation by the CFSV2 model indicated that the dynamical consistency of both the forecast and the predictability error are purely systematic in nature, and improvement of the physical processes in the CFSv2 may enhance the overall predictability (Pokhrel et al. 2016). The actual skill of CFSv2 in predicting ISMR is very close to the potential predictability limit (Saha et al. 2016). Despite the improvement in the performance of the coupled models, the skill of predicting ISMR by these models is not, as yet, adequate.

The role of ocean–atmosphere coupling in improving the skill of predicting the monsoon intraseasonal oscillations (MISOs) using NCEP CFSv2 and its atmospheric component GFS with bias-corrected SST from CFSv2-predicted SST has been investigated (Sahai et al. 2013). Sahai et al. pointed out that the improvement of MISO simulation in CFS over GFS has not improved the real-time extended prediction during 2011 and 2012. A lead time-dependent SST bias correction that forced the GFS (atmospheric component of CFSv2) with slightly different physics was implemented and showed that it has improved skill over India compared to the CFSv2. The potential predictability limit is comparable (~ 16 days) for both bias-corrected GFSv2 (GFSv2bc) and CFSv2. Skill at predicting active and break spells and of low-frequency MISOs is higher for GFSv2bc at all lead pentads. Although initially the same, the predictability error after 14 days grows slightly faster for GFSv2bc compared

to CFSv2. Bias correction in SST has minimal impact in the short to medium range, while substantial influence is felt in the extended range between 12 and 18 days (Abhilash et al. 2014). The uncoupled AGCM with the bias-corrected SST is able to leverage the teleconnection for improved skill of seasonal prediction of the South Asian monsoon relative to the coupled models which display large systematic errors of the tropical SSTs (Misra and Li 2014).

Since 2005, the Centre for Development of Advanced Computing (C-DAC) has been a part of seasonal forecast of ISMR using the NCEP's T170/L42 Atmospheric Global Circulation Model (AGCM). The normal monsoon during 2005 was well forecasted by the model (Ratnam et al. 2007). Furthermore, the model is employed to simulate the past 20 years of monsoon using observed SST as boundary conditions. It is found that interannual variability, as well as model-simulated climatology for circulation and ISMR, are in good agreement with observations, suggesting that model can become a good tool for dynamical long-range monsoon prediction with initial condition in the beginning of May using five ensemble members (Ratna et al. 2011). In a separate study, it was found that the success of long-range seasonal dynamical forecast by SST forcing depends on the predictability of tropical SST anomalies both over the equatorial Pacific Ocean (ENSO signal) as well as over the Eastern Indian Ocean (IOD/EQUINOO signal). This shows the influence of IOD as well as Equatorial Indian Ocean Oscillation (Gadgil 2003). It is vital to investigate the important air–sea interactions by exploring the relationship of SST–rainfall in the coupled CFSv2 model, in which CFSv2-predicted SST is used as input for the T170 AGCM model. The question remains unanswered how SST of different regions and ISMR are related in this model by forcing with CFSv2-predicted SST and a bias-corrected SST as compared to observed SST. The present study is an attempt to answer the above question.

In this study, the CFSv2 model climatology of ISMR and SST are analysed to examine the accuracy of CFSv2, from which SST will be used as boundary forcing for the T170 model. SST–rainfall correlation is examined for the air–sea interactions in the CFSv2 model. The interannual variability of the ENSO-ISMR and IOD-ISMR relations in the CFSv2 simulations is analysed for the three different periods (1985–2009, 1985–1998 and 1999–2009). Determining the sensitivity of the NCEP GFS (T170) model to SST boundary forcing in ISMR prediction is carried out with CFSv2-predicted SST and the National Oceanic and Atmospheric Administration's (NOAA's) optimum interpolated SST (OISST). The next section will discuss the data and methodology used in this study.

1.1. Data and Methodology

The NCEP GFS is a moderate-resolution general circulation model. In this study, the NCEP T170/L42 AGCM is configured with horizontal resolution of 75×75 km, with 42 vertical sigma levels. The relaxed Arakawa-Schubert scheme was used for cumulus parameterization, the Rapid Radiation Transfer Model (RRTM; Mlawer et al. 1997) scheme was used for long-wave radiation, the Troen and Mahrt (1986) scheme was used for planetary boundary layer (PBL) and the Pan and Mahrt 1987 scheme was used for land surface processes. The initial conditions were derived from NCEP re-analysis-II data (Kanamitsu et al. 2002). The slowly varying boundary values of SST were derived from the output of the NCEP CFSv2 re-forecasts (Saha et al. 2010) and observed global SST (Reynolds et al. 2002). The monthly forecasted SST of the NCEP CFS system and observed SST was used as input boundary forcing for model simulations. NCEP provides forecasts of SST using a coupled CFSv2 system.

The atmospheric component of CFSv2 consists of a spectral atmospheric GFS model at a high resolution of T126 with 64 hybrid vertical levels, and the oceanic component, Modular Ocean Model (Griffies et al. 2004) is used. It uses the SAS convection scheme with momentum fixing, the rapid and accurate radiative transfer model (RRTM) shortwave radiation scheme with maximum random cloud overlap (Iacono et al. 2000; Clough et al. 2005), the four-layer Noah land surface model (Ek et al. 2003) and a two-layer sea ice model based on Wu et al. (1997) and Winton (2000). Initial conditions for the atmosphere and ocean are from the NCEP Climate

Forecast System Reanalysis (CFSR) (Saha et al. 2010).

An ensemble of the model seasonal runs was made using the initial conditions of May 1st to May 5th. The model was run for 31 years (from 1985 to 2015) with forecast SST and observed SST. The model-simulated rainfall is compared with India Meteorological Department (IMD) observed gridded rainfall (Rajeevan et al. 2005). The CFSv2 forecast SST are compared with NOAA's OISST (data acquired from NOAA_OI_SST_V2 data products).

The climatology of rainfall and SST during monsoon (June through September) season for 25 years from (1985–2009) is calculated from observed IMD gridded rainfall data and OISST data, respectively. The performance of the CFSv2 model is evaluated in terms of climatological rainfall bias and SST bias (model minus observation) with respect to observations for the same period. Also evaluated was the skill and prediction ability of the model regarding the 1999 discontinuity in the initial conditions due to CFSR (Kumar et al. 2012), associated with the use of Advanced Television Infrared Observation Satellite (TIROS) Operational Vertical Sounder (ATOVS) radiance data. Hence, the significance of discontinuity is assessed based on the two-period approach of climatology over the years 1985–1998 and 1999–2009 separately. The SST bias and rainfall bias is computed by removing modelled climatology and observed climatology for the two time scales 1985–1998 and 1999–2009. The interannual variability of rainfall and SST indices (Nino 3 and IOD) of CFSv2 is examined with respect to observations. Nino 3 indices are calculated as the area-averaged SST over the Nino 3 region (5°N–5°S, 150°–90°W). The IOD has been calculated as the difference in the anomaly of SSTs over the western equatorial Indian Ocean and that over eastern equatorial Indian Ocean and is compared with the observations.

The systematic model-forecasted SST bias leads to poor amplitude of convective precipitation. This bias can be effectively reduced with statistical correction. Bias correction in daily forecasted SST from CFSv2 for each lead time has been calculated by removing the daily mean bias for corresponding lead time from forecasted daily SST. The bias-corrected SST is used as the boundary forcing for the

GFS-T170 model in one experiment. The T170 model simulations with bias-corrected SST are carried out for a simulation period of May to September using May initial conditions. These simulations are conducted for the years 1985 to 2015 and are evaluated with CFSv2-predicted SST and OISST. Summer monsoon rainfall bias as simulated by the GFS model forced with observed SST, CFSv2-predicted SST and CFSv2 bias-corrected SST are analysed for the periods 1985–2009, 1985–1998 and 1999–2009. Also, the interannual variability of ISMR is evaluated with respect to observations for these three sets of experiments.

2. Results and Discussion

2.1. Simulation of ISMR by the NCEP CFSv2 Model

2.1.1 Monsoon Climatology

The climatological ISMR for a period of 25 years (1985–2009) from IMD observations is shown in Fig. 1a. The observed climatological mean ISMR is characterized by three convection zones; western coast of India, Central India and North-east India. CFSv2 bias of predicted climatological mean ISMR for the same period is presented in Fig. 1c. The state-of-art coupled CFSv2 model simulates climatological mean ISMR quite well with a dry bias over Western India. The model simulated mean summer rainfall with a significant dry bias over all the three convection zones; Western Ghat, North-east India and Central India. The dry bias over the Indian land mass is not unique to the CFSv2 model, but many CMIP5 models have also shown a similar bias in the precipitation simulation (Sabeerali et al. 2013; Sahai et al. 2013). A dry bias of −5 mm/day is depicted over Western Ghat and north-east regions. The dry bias over Central India reduced westward to the north-west states, from Orissa, Madhya Pradesh and Rajasthan, varying over a range of −5 to −1 mm/day. The model realistically simulated rainfall over south-eastern peninsular India.

To check the dependency of the rainfall prediction skill on the initial conditions of SST boundary
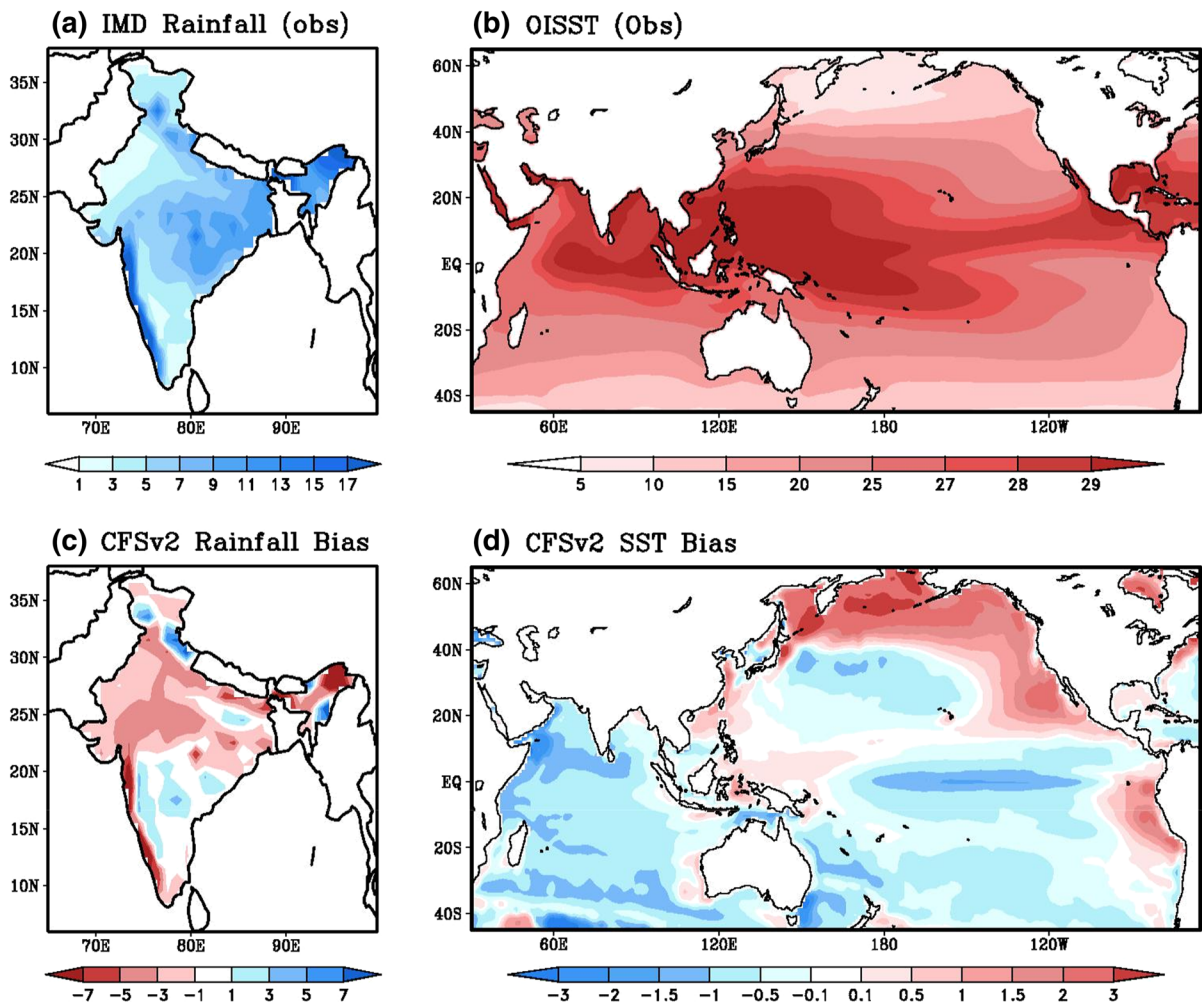
Figure 1
Observed climatology of summer monsoon **a** rainfall and **b** SST. Bias of the CFSv2 model in simulating the climatological **c** rainfall and **d** SST. Both the observation and model simulation are based on 25 years (1985–2009) of climatology

forcing, the climatological SST for the same period is analysed. Figure 1b represent climatological June–July–August–September (JJAS) mean SST from Reynold's SST observations. The model simulated large cold bias in the central equatorial Pacific Ocean and Indian Ocean (Fig. 1d) as compared to observed climatological mean OISST (Fig. 1b). The CFSv2 model simulated cold bias over the Indian Ocean basin and central equatorial Pacific, with strong cold bias over a narrow region of the eastern equatorial Pacific Ocean. Cold SST bias over the equatorial Indian Ocean co-occurs with strong easterlies as compared to observations (Seo et al. 2007). A

significant warm bias is simulated over the North Pacific Ocean, which might be due to the misrepresentation of stratus cloud decks in the eastern Pacific and the resulting penetration of more shortwave radiation to the surface, as reported by Zheng et al. (2011). The SST bias over the two basins of the Arabian Sea and Bay of Bengal has a greater impact on the ISMR. The significant cold bias over the Arabian Sea might have affected the model adversely for the simulation of ISMR. This indicates the model's reduced efficiency in capturing the mixing, evaporation and radiation fluxes associated with the SST simulation.
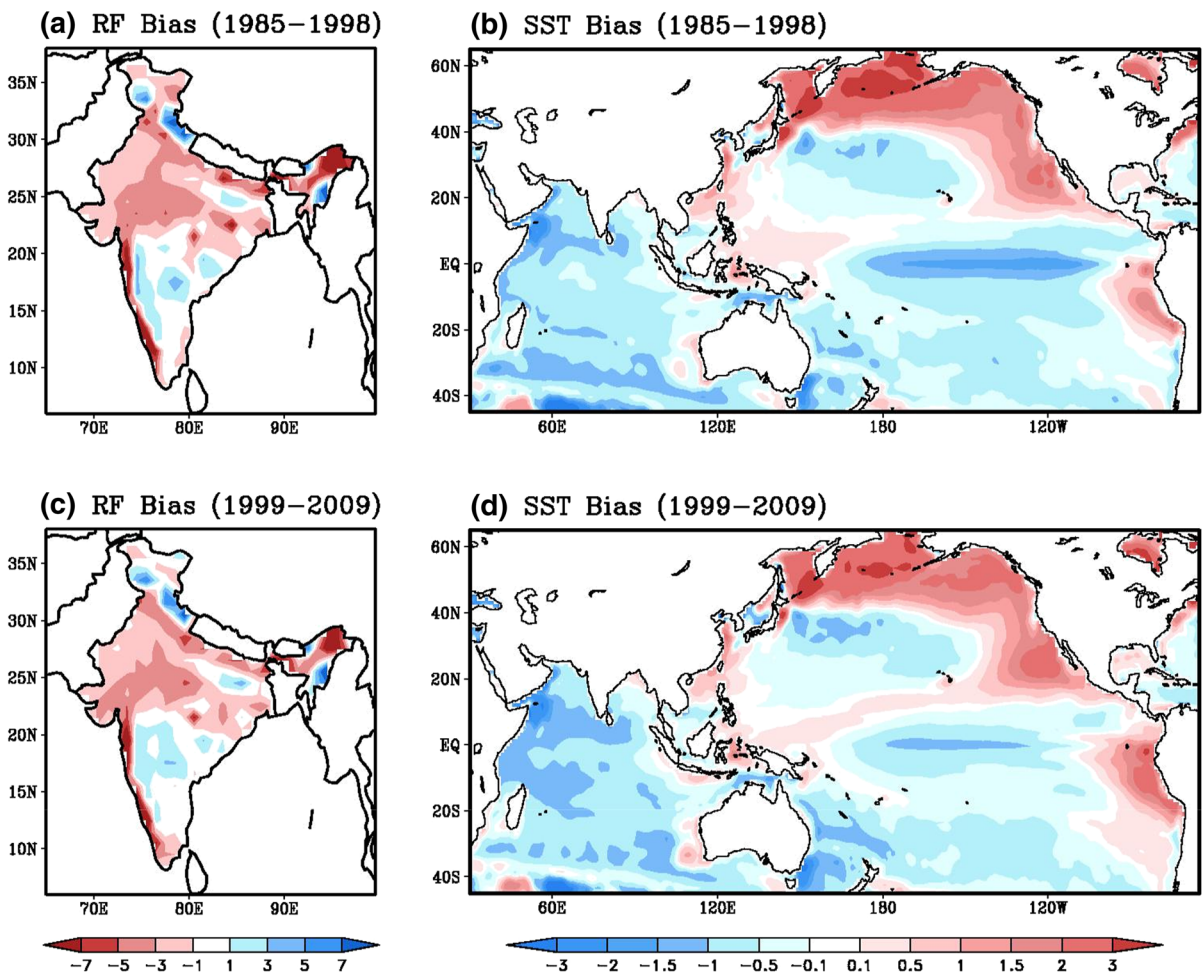
Figure 2
CFSv2 bias in simulating mean summer monsoon **a**, **c** rainfall and **b**, **d** SST for two different periods: **a**, **b** 1985–1998 and **c**, **d** 1999–2009

The improvement in CFSv2 associated with the 1999 discontinuity in the initial conditions is verified based on the two-period approach; 1985–1998 and 1999–2009. The CFSv2 model-simulated ISMR bias remained the same as climatology with a dry bias for both periods of 1985–1998 and 1999–2009 (Fig. 2a, c). In contrast, there is significant improvement in the cold bias of central equatorial Pacific Ocean SST during the 1999–2009 period as compared to the previous period and 25 years of climatology. Further, cold bias over Indian Ocean SST has increased during this period as compared to earlier climates (Fig. 2b and 2d).

2.1.2 Interannual Variability

During the study period, ISMR has seen two flood years (1988 and 1994) and six drought years (1985, 1986, 1987, 2002, 2004 and 2009). IMD considers a drought year as an anomaly below –10% of normal and a flood year as an anomaly above 10% of normal rainfall. The interannual variability of ISMR is studied using IMD observations and evaluated by the CFSv2 model performance for the period 1985–2009; the results are presented in Fig. 3a. The standardized rainfall anomaly of the model and observed data is compared in Fig. 3a. The model could correctly capture 64% (16 out of 25) of the year's rainfall anomaly signal (positive or negative).
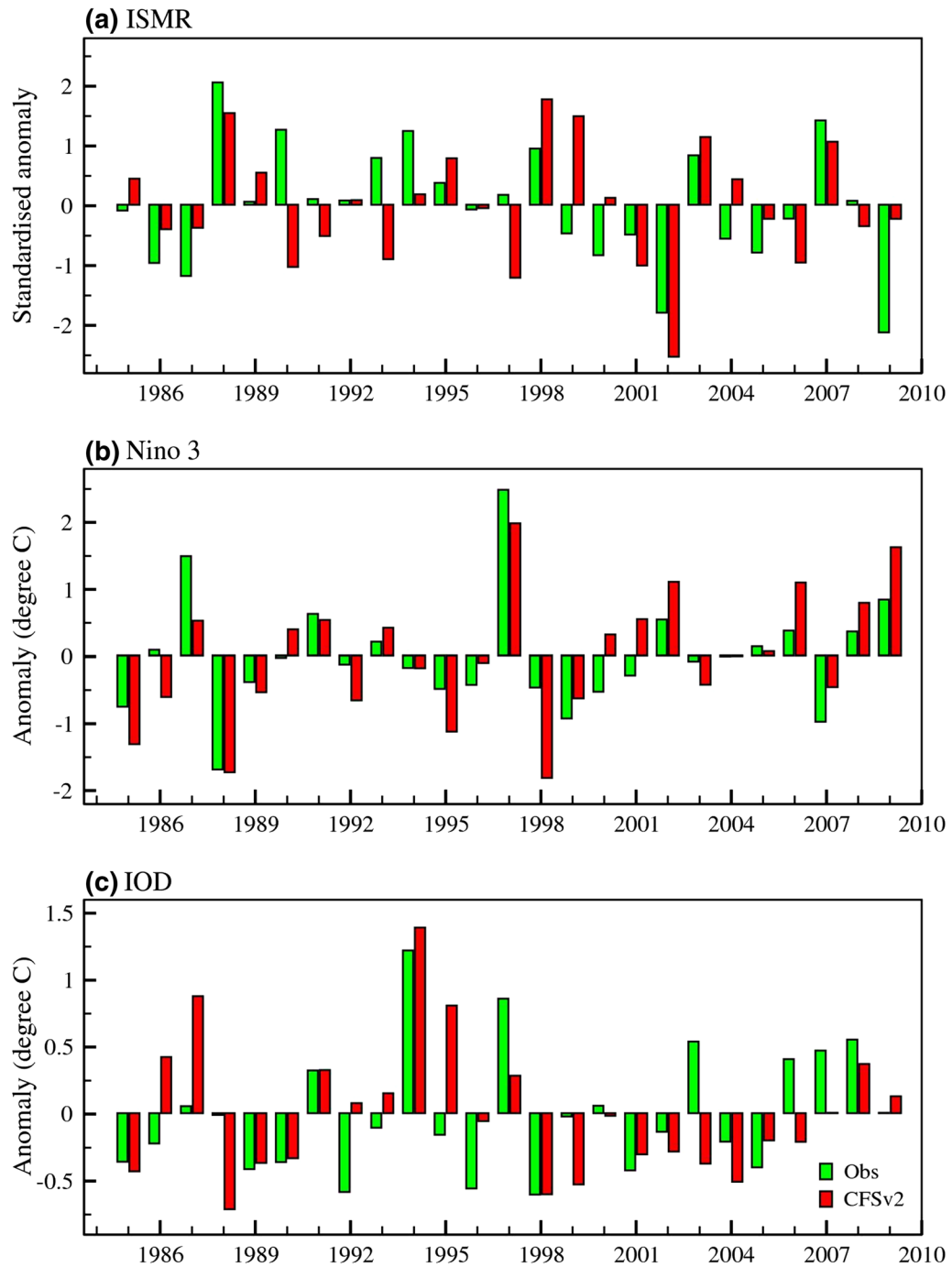
Figure 3
Interannual variability of rainfall and SST indices from observation (green bars) and CFSv2 model simulation (red bars) for the period 1985–2009. **a** ISMR, **b** Niño 3 and **c** IOD indices. The rainfall anomalies from observation and model simulation in **a** are normalised by their respective standard deviation for the 25-year period

The model simulated flood years like 1988 and 1994 well with a positive anomaly. The model could capture the negative anomaly for all other drought years, except for 1985. The accuracy of the model-simulated ISMR is improved in recent years, which is evident from correlation with observed rainfall with correlation coefficients of 0.46 (1985–2009), 0.35 (1985–1998) and 0.58 (1999–2009). The model simulated a negative mean bias (underestimate) in the ISMR during all periods (dry bias evidence from Fig. 1).

The standardized SST anomaly during JJAS (monsoon months) of the Nino 3 region for model simulation and OISST observation are shown in Fig. 3b. Out of 25 years, the model showed a similar sign (positive or negative) for 19 years (76%) in comparison with observations. The anomalous cooling in 1988 and warming in 1997 (super-El Nino year) were well-captured by model simulation. The interannual variability of the Nino 3 index and its impact on droughts and excess rainfall seasons can be distinguished. The El Nino event of 1987 was associated with drought, and the La Nina event of 1988 with excess rainfall. The super-El Nino during 1997 resulted in normal ISMR, which is an exception in terms of the relationship between monsoon and ENSO. The model could simulate the negative Nino 3 and excess rainfall and the La Nina event realistically for the year 1988. The model shows a large difference in Nino indices for the years 1987 and 1998, which led to the unrealistic rainfall simulation. Contrary to observations, CFSv2 shows an intense warming in the Nino 3 region; however, it could not capture the deficit of ISMR in the year 2009.

The IOD plays an important role as a modulator of the ISMR and influences the correlation between the ISMR and ENSO. The standardized SST anomaly of the IOD index during JJAS for model simulation and OISST observation are shown in Fig. 3c. Of the 25 years, the model showed a similar sign (positive or negative) for 18 years in comparison with observations. The anomalously positive IOD in 1994 is well-captured by model simulation, whereas the negative IOD year of 1998 could be simulated well; but simulation failed for the years 1992 and 1996. During the super-El Nino year of 1997, a favourable positive IOD index and an enhanced equatorial Indian Ocean

oscillation are observed, which led to normal monsoon rainfall. The model could simulate a positive IOD, but simulated a deficit ISMR as a result of the strong El Nino event. The model failed to produce the IOD indices correctly for the years 1986, 1987 and 1995. The correlation of model-simulated IOD with respect to observations suggests a low score (0.3) during the recent period of 1999–2009 as compared to an earlier period (1985–1998) and the mean. It is noticed the model has low skill at indicating the IOD and ISMR relationship.

2.1.3 Monsoon Teleconnections

ISMR is sensitive to seasonal variations of Pacific Ocean SST, with a tendency for below (above) normal monsoon rainfall to occur during El Nino (La Nina). Also, this is proved using the GCM and observational data (Shukla and Huang 2015; Shukla and Misra 1977), in which ISMR was found to be positively correlated with the SST anomalies over the Arabian Sea. The ENSO-monsoon teleconnections are evaluated using CFSv2 simulation as a comparison with observations. The observed relationship between ISMR and SST for the periods 1985–2009, 1985–1998 and 1985–2009 are represented in Fig. 4a–c. The correlation coefficients between the JJAS SST and ISMR are evaluated using observations. A strong negative correlation is seen over the central equatorial Pacific, and positive correlation is seen along the South and East China Sea. A negative correlation indicates colder (warmer) SST will increase (decrease) ISMR. The strengthening of correlation occurred in the recent period of 1999–2009. During the recent period, a negative correlation is observed in the Bay of Bengal region, whereas the negative correlation in the south equatorial Indian Ocean disappears in the later period. Contrary to observations, the CFSv2 model simulated a high correlation in the earlier period (1985–1998) than the recent period (Fig. 4d–f). The CFSv2 model simulated a stronger positive correlation along the China Sea and stronger negative correlation in the central equatorial Pacific, compared to observations. This conclude the strong ENSO-monsoon teleconnection in the CFSv2 model; hence, an accurate simulation of ENSO SST is necessary for the realistic
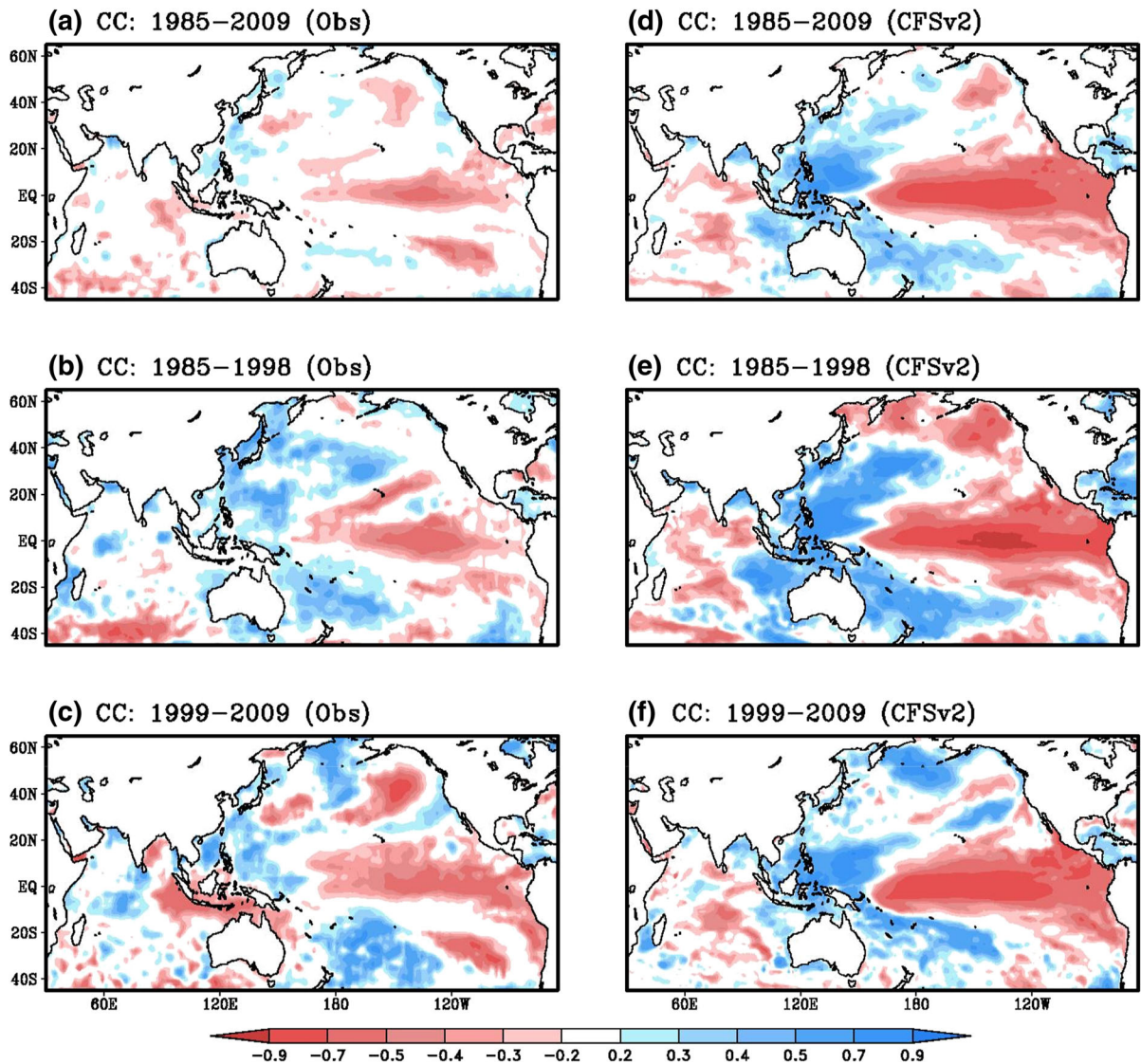
Figure 4
Correlation between ISMR and summer monsoon sea surface temperature from **a–c** observation and **d–f** CFSv2 simulations, for the periods **a**, **d** 1985–2009, **b**, **e** 1985–1998 and **c**, **f** 1999–2009

simulation of ISMR. Regarding one more important IOD teleconnection, in recent years (1999-2009), observations (Fig. 4c) have a strong negative correlation with ISMR in the eastern equatorial Indian Ocean, whereas the model is missing that signature (Fig. 4f).

The correlation coefficients between the SST in the Nino 3 region of the JJAS season and ISMR are evaluated for the CFSv2 model and observations (Fig. 5). The observed relationship between Nino 3

index and ISMR is represented in Fig. 5a–c for all three time scales (1985–2009, 1985–1998 and 1999–2009). A negative correlation is observed along the north and southern peninsular India, except for a few parts of Jammu Kashmir and Western Ghats. Stronger correlation is observed during the earlier time scale (1985–1998) as compared to the recent period. During the earlier period, a significant positive correlation was observed over the states of Bihar, Jharkhand and West Bengal, while a negative
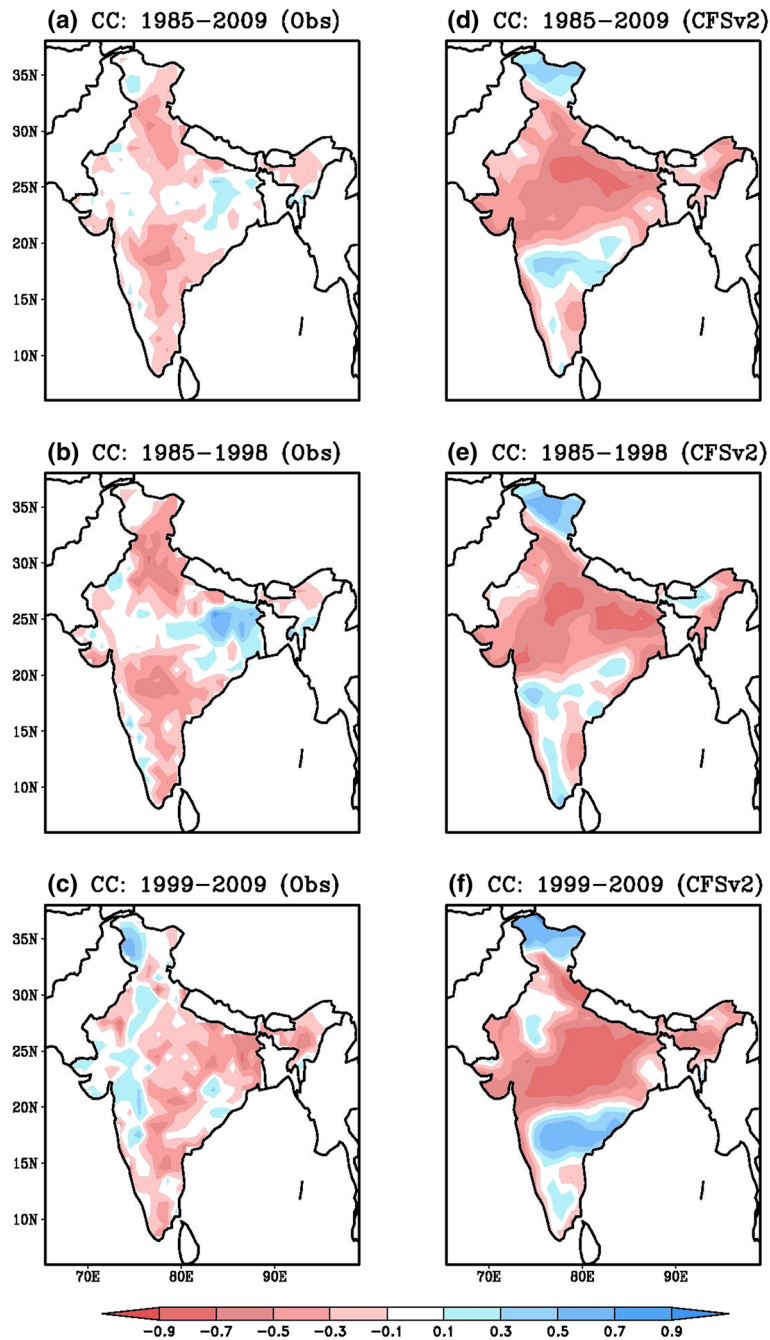
Figure 5

Correlation between Niño 3 index and ISMR from **a–c** observation and **d–f** CFSv2 simulations, for the periods **a**, **d** 1985–2009, **b**, **e** 1985–1998 and **c**, **f** 1999–2009

correlation was observed for the same region during the recent period. The correlation of CFSv2 model-simulated Nino 3 and ISMR is shown in Fig. 5d–f.

The model simulated a significant negative correlation over the whole of Central India and North-east India, with a positive correlation over Jammu
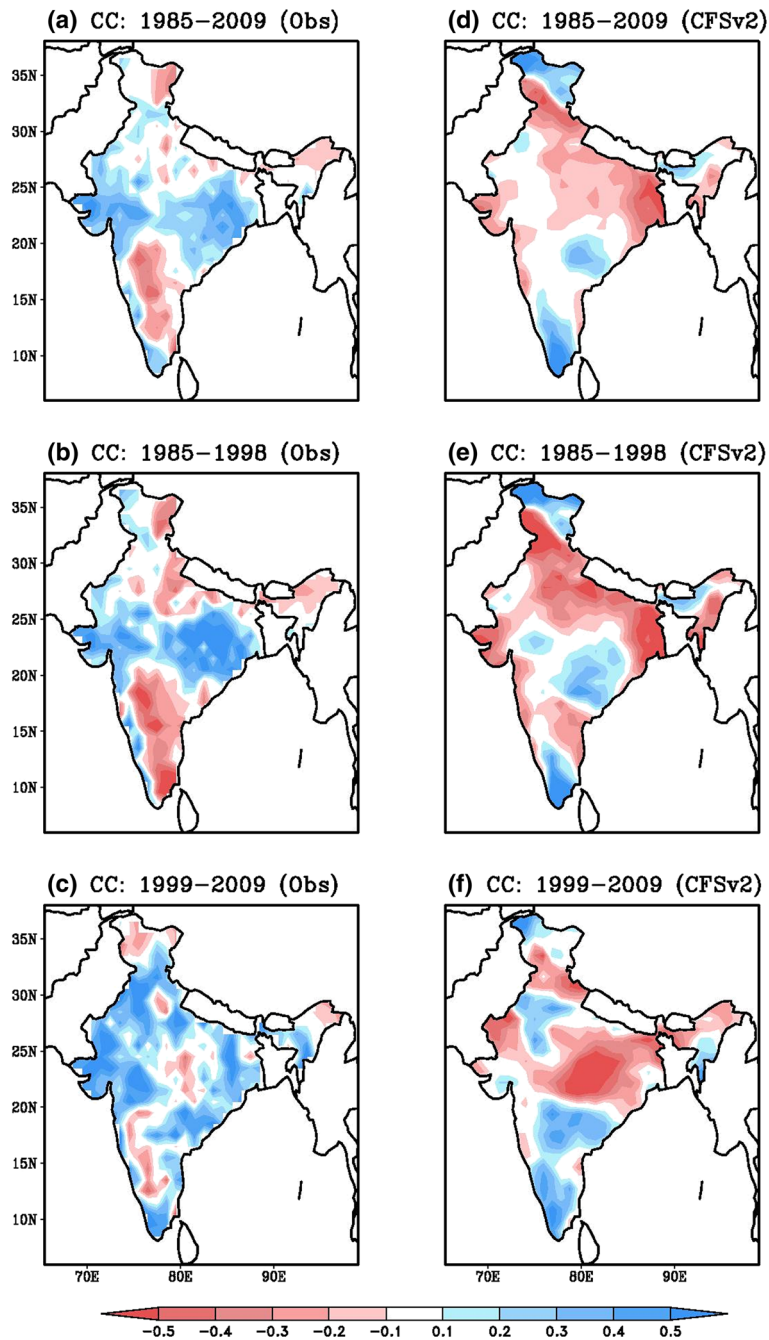
Figure 6
Same as Fig. 5, but for IOD index

Kashmir for all three time scales. Model simulation shows a stronger correlation during the recent period as compared to the earlier period.

The relation of IOD index and ISMR from observations and model simulation for the three climatological periods is shown in Fig. 6. It is found the correlations are poor and spatially varying from

the earlier period to the recent period. Similarly, model-simulated correlations are inconsistent with observations. This indicates ENSO impacts are more strongly correlated with ISMR as compared to IOD. The correlation of ISMR with different SST indices is computed for observations and the CFSv2 model (Table 1). ISMR in the recent period (1999–2009) has seen a strong positive correlation with IOD, and strong negative correlation with Nino 3 in the observations. The CFSv2 model could not capture those correlations realistically; this suggests the improvement in SST simulation in the CFSv2 model.

2.2. Simulation of ISMR by the GFS-T170 Model

2.2.1 Monsoon Climatology

To study the impact of SST for ISMR simulation by the high-resolution NCEP T170 AGCM is employed. The model simulated ISMR for 1985 to 2009 during JJAS with three different SST boundary forcings. Three experiments are conducted, first with observed SST (OISST), second with CFSv2-simulated SST and third with CFSv2 bias-corrected SST. The model-simulated ISMR bias as compared to observation is presented for all three time periods and all three experiments (Fig. 7). The model forced with observed SST shows wet bias in peninsular India and dry bias over North-east India (Fig. 7a–c). The model forced with CFSv2-predicted SST simulated a wet bias in peninsular India and wide spread dry bias in North and Central India (Fig. 7d–f). In the third

experiment, when the model was forced with bias-corrected CFSv2 SST, the dry bias improved in North and Central India, whereas the intensity of wet bias increased in peninsular India (Fig. 7g–i). No significant improvement in bias is noticed for the different time periods for all SST boundary forcing.

2.2.2 Interannual Variability

The interannual variability of ISMR is studied using IMD observations, and the T170 model performance is evaluated for the period 1985–2009, as represented in Fig. 8a–c, for all three forcing experiments. The rainfall anomalies from observation and model simulations are normalized by their respective standard deviation. The standardized rainfall anomaly of model-simulated and observed data are compared for forced simulation with observed SST, CFSv2-predicted SST and bias-corrected CFSv2 SST in Fig. 8a–c, respectively. It is noticed the model could capture 56, 48 and 64% of the year's rainfall anomaly signal (positive or negative) correctly in the same sign for forced simulation with observed SST, CFSv2-predicted SST and bias-corrected CFSv2 SST, respectively. All three experiments simulated the 1988 flood year, whereas for the 1994 flood year, only the bias-corrected CFSv2 SST experiment (Fig. 8c) simulated the correct signature. For drought years like 2002 and 2009, the first experiment with observed SST could simulate both droughts, whereas the second experiment with CFSv2-predicted SST failed to capture the 2009 drought; and the third experiment with bias-corrected CFSv2 SST failed to

Table 1

Correlation of ISMR with SST indices

	IODM	Nino 4	Nino 3.4	Nino 3	Nino 2	Nino 1
Observed correlation coefficient						
1985–2009	0.23	− 0.34	− 0.47	− 0.44	− 0.14	− 0.11
1985–1998	0.16	− 0.37	− 0.54	− 0.49	− 0.23	− 0.17
1999–2009	0.62	− 0.33	− 0.33	− 0.60	− 0.32	− 0.46
Observed correlation coefficient						
1985–2009	− 0.23	− 0.78	− 0.84	− 0.78	− 0.66	− 0.62
1985–1998	− 0.36	− 0.81	− 0.91	− 0.90	− 0.83	− 0.70
1999–2009	− 0.16	− 0.78	− 0.84	− 0.77	− 0.56	− 0.58

GFS: Obs_SST

(a) 1985−2009

GFS: CFSv2_SST

(d) 1985−2009

GFS: CFSv2_SSTbc

(g) 1985−2009

(b) 1985−1998

(e) 1985−1998

(h) 1985−1998

(c) 1999−2009
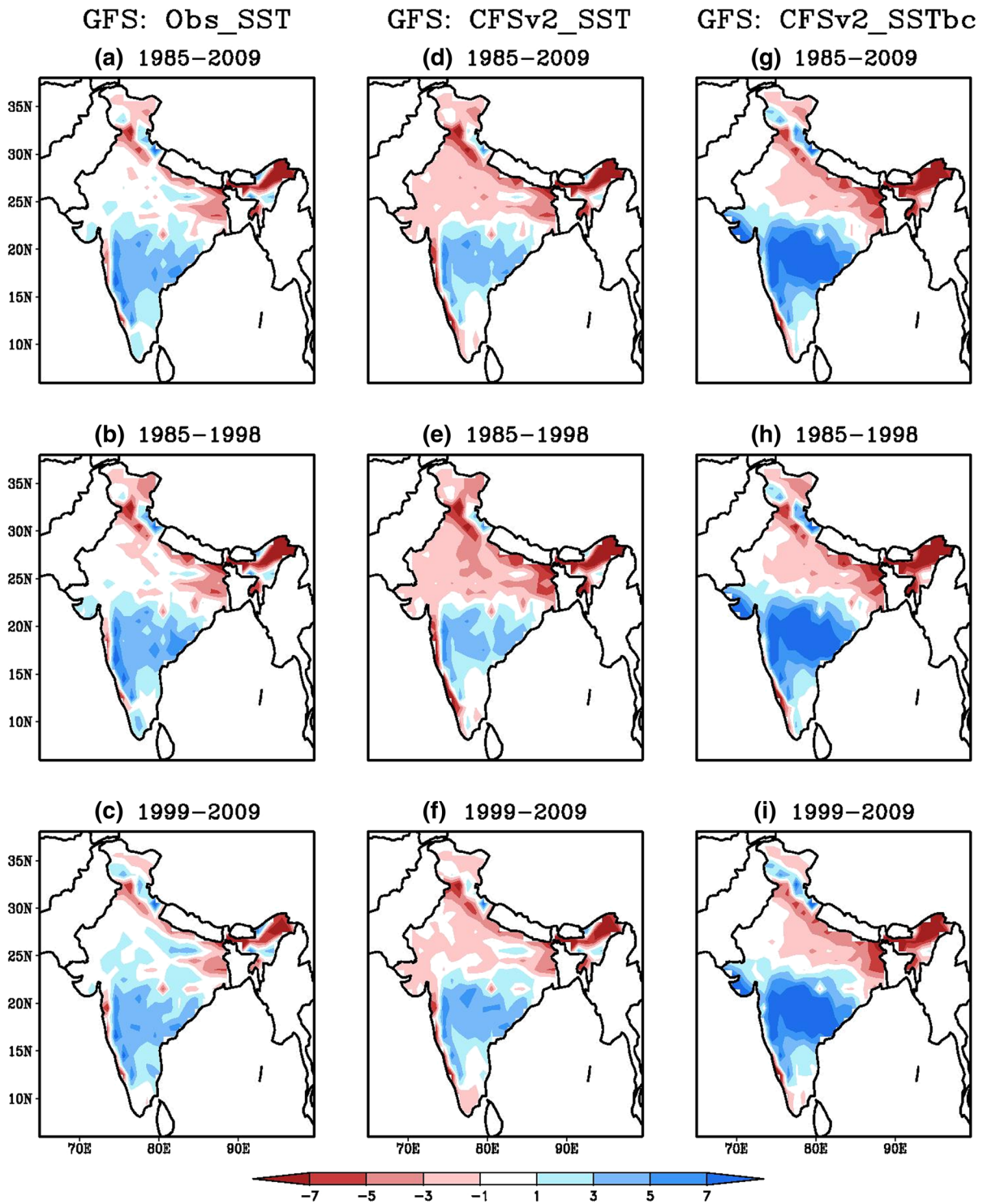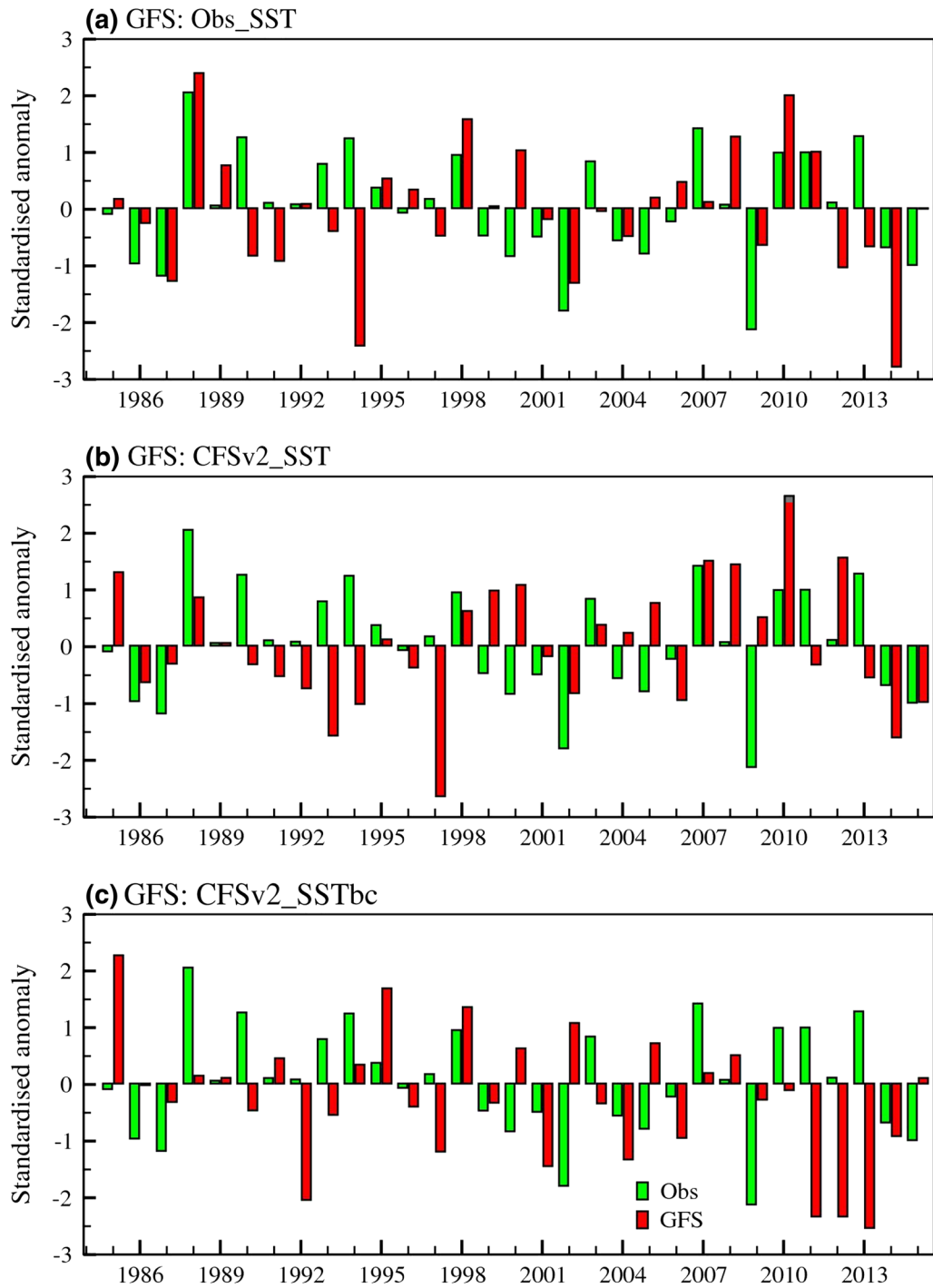
(f) 1999−2009

(i) 1999−2009

Figure 7
ISMR bias as simulated by the GFS model forced with **a–c** observed SST, **d–f** CFSv2-predicted SST and **g–i** CFSv2 bias-corrected SST, for the periods **a**, **d**, **g** 1985–2009, **b**, **e**, **h** 1985–1998 and **c**, **f**, **i** 1999–2009

Figure 8
Interannual variability of ISMR as simulated by the GFS model forced with **a** observed SST, **b** CFSv2-predicted SST and **c** CFSv2 bias-corrected SST, along with observed ISMR. The rainfall anomalies from observation and model simulations are normalised by their respective standard deviation

simulate the 2002 drought. The correlation skill of the T170 model with observed rainfall shows improvement in the recent period (1999–2009) for all three SST input forcings. This indicates the importance of SST forcing in the model, and requires further sensitivity study to improve ISMR simulation.

3. Conclusion

The slowly varying SST boundary forcing plays a major role in the skill of predicting ISMR, but remains a challenge for AGCMs. In this study, the SST–rainfall relationship is examined in the coupled CFSv2 model, in which CFSv2-predicted SST is used as input for the AGCM. The NCEP T170/L42 AGCM configured with horizontal resolution of 75×75 km, with 42 vertical levels is used for the study. The performance of CFSv2 is evaluated in terms of climatological rainfall and SST, and the interannual variability of rainfall and SST indices, with observations. The atmospheric NCEP GFS-T170 simulations are carried out with boundary forcing of observed SST, CFSv2-predicted SST and the bias-corrected CFSv2 SST. An ensemble of seasonal runs was made using the initial conditions of May to September. The Indian summer monsoon season for the climatological period of 1985-2009 is considered for the study. The significance of discontinuity in the initial conditions due to CFSR is assessed based on the two-period approach of climatology for the two time scales (1985–1998 and 1998–2009).

Similar to other studies related to CFSv2, the model simulated mean summer rainfall with a significant dry bias over the three convection zones; Western Ghats, Central India and North-east India. CFSv2 predicted cold bias over the Indian Ocean basin and central equatorial Pacific, with strong cold bias over a narrow region of equatorial Pacific. The model could capture 64% (16 out of 25) of the year's rainfall anomaly signal. The skill of the model is improved in recent years. The model could simulate the negative Nino 3 and excess rainfall and the La Nina event realistically for the year 1988. The model shows a large difference in Nino indices for the years 1987 and 1998, which led to the unrealistic rainfall simulation. It is noticed the model has a low skill at at

indicating the IOD and ISMR relationship. The CFSv2 model simulated a stronger positive correlation along the China Sea and stronger negative correlation in the central equatorial Pacific, compared to observations. This indicates the strong ENSO-monsoon teleconnection in the CFSv2 model; hence, an accurate simulation of ENSO SST is necessary for the realistic simulation of ISMR. Regarding one more important IOD teleconnection, in recent years (1999-2009), observed correlations have seen a strong negative correlation with ISMR at East Equatorial Indian Ocean, whereas the model is missing that signature. The correlation between Nino 3 index and ISMR shows that model simulated a significant negative correlation over the whole of Central India and North-east India, while simulating a positive correlation over Jammu Kashmir for all three-time scales. Model simulation shows a stronger correlation during the recent period as compared to the earlier period, whereas model-simulated correlation between IOD index and ISMR is inconsistent with observations. ISMR in the recent period (1999–2009) has seen a strong positive correlation with IOD and strong negative correlation with Nino 3 in the observation. The CFSv2 model could not capture those correlations realistically; this suggests the improvement in SST simulation in the CFSv2 model.

The impact of SST for ISMR simulation by the high-resolution NCEP T170 AGCM model is analysed with observed SST, CFSv2-predicted SST and bias-corrected CFSv2 SST in comparison with observations. The model forced with observed SST shows wet bias in peninsular India and dry bias over North-east India. The model forced with CFSv2-predicted SST simulated a wet bias in peninsular India and widespread dry bias in North and Central India. In the third experiment, when the model was forced with bias-corrected CFSv2 SST, the dry bias improved in North and Central India, whereas the intensity of wet bias increased in peninsular India. The model could capture 56, 48 and 64% of the year's rainfall anomaly signal (positive or negative) correctly in the same sign for forcing with observed SST, CFSv2-predicted SST and bias-corrected CFSv2 SST, respectively. All three experiments simulated the 1988 flood year, whereas the 1994 flood year was simulated with the correct signature

only by the bias-corrected CFSv2 SST experiment. For drought years like 2002 and 2009, the first experiment with observed SST could simulate both droughts, whereas the second experiment with CFSv2-predicted SST failed to capture the 2009 drought; the third experiment with bias-corrected CFSv2 SST failed to simulate the 2002 drought case. This indicates the importance of SST forcing in the model. Further sensitivity study is required to improve ISMR simulation.

Acknowledgements

Publisher's Note   Springer Nature remains neutral with regard to jurisdictional claims in published maps and institutional affiliations.

References

Abhilash, S., Sahai, A. K., Borah, N., Chattopadhyay, R., Joseph, S., Sharmila, S., et al. (2014). Does bias correction in the forecasted SST improve the extended range prediction skill of active-break spells of Indian summer monsoon rainfall? *Atmospheric Science Letters, 15,* 114–119. https://doi.org/10.1002/asl2.477.

Abhilash, S., Sahai, A. K., Pattnaik, S., Goswami, B. N., & Kumar, A. (2013). Extended range prediction of active-break spells of Indian summer monsoon rainfall using an ensemble prediction system in NCEP climate forecast system. *International Journal of Climatology.* https://doi.org/10.1002/joc.3668.

Azad, S., & Rajeevan, M. (2016). Possible shift in the ENSO-Indian monsoon rainfall relationship under future global warming. *Scientific Reports, 6,* 20145. https://doi.org/10.1038/srep20145.

Bollasina, M. A., & Nigam, S. (2009). Indian Ocean SST, evaporation and precipitation during the South Asian summer monsoon in IPCC-AR4 coupled simulations. *Climate Dynamics, 33,* 1017–1032.

Chattopadhyay, R., Rao, S. A., Sabeerali, C. T., George, G., Rao Nagarjuna, D., Dhakate, A., et al. (2016). Large-scale teleconnection patterns of Indian summer monsoon as revealed by CFSv2 retrospective seasonal forecast runs. *International Journal of Climatology, 36,* 3297–3313. https://doi.org/10.1002/joc.4556.

Chaudhari, H. S., Pokhrel, S., Saha, S. K., Dhakate, A., Yadav, R. K., Salunke, K., et al. (2013). Model biases in long coupled runs of NCEP CFS in the context of Indian summer monsoon. *International Journal of Climatology, 33,* 2013. https://doi.org/10.1002/joc.3489,1057-1069.

Clough, S. A., Shephard, M. W., Mlawer, E. J., Delamere, J. S., Iacono, M. J., Cady-Pereira, K., et al. (2005). Atmospheric radiative transfer modeling: A summary of the AER codes. *Journal of Quantitative Spectroscopy & Radiative Transfer, 91,* 233–244.

Drbohlav, H.-K. L., & Krishnamurthy, V. (2010). Spatial structure, forecast errors, and predictability of the South Asian Monsoon in CFS monthly retrospective forecasts. *Journal of Climate, 23,* 4750–4769. https://doi.org/10.1175/2010JCLI2356.1.

Ek, M. B., Mitchell, K. E., Lin, Y., Rogers, E., Grunmann, P., Koren, V., et al. (2003). Implementation of Noah land surface model advances in the National Centers for environmental prediction operational mesoscale Eta model. *Journal of Geophysical Research, 1089*(D22), 8851. https://doi.org/10.1029/2002JD003296.

Gadgil, S. (2003). The Indian monsoon and its variability. *Annual Review of Earth and Planetary Sciences, 31,* 429–467.

Gadgil, S., Rajeevan, M., & Nanjundiah, R. S. (2005). Monsoon prediction—why yet another failure? *Current Science, 88,* 1389–1400.

Gadgil, G., & Sajini, S. (1998). Monsoon precipitation in the AMIP runs. *Climate Dynamics, 14,* 659–689.

Ganai, M., Mukhopadhyaya, P., Krishna, R. P., & Mahakur, M. (2015). Impact of revised simplified Arakawa-Schubert convection parameterization scheme in CFSv2 on the simulation of the Indian summer monsoon. *Climate Dynamics, 45,* 881–902. https://doi.org/10.1007/s00382-014-2320-4.

George, G., Rao, D. N., Sabeerali, C. T., Srivastava, A., & Rao, S. A. (2016). Indian summer monsoon prediction and simulation in CFSv2 coupled model. *Atmospheric Science Letters, 17,* 57–64. https://doi.org/10.1002/asl.599.

Goswami, B. B., Deshpande, M. S., Mukhopadhyay, P., Saha, Subodh K., Rao, Suryachandra A., Murthugudde, R., et al. (2014a). Simulation of monsoon intraseasonal variability in NCEP CFSv2 and its role on systematic bias. *Climate Dynamics, 43,* 2014. https://doi.org/10.1007/s00382-014-2089-5,2725-2745.

Goswami, B. B., Deshpande, M., Mukhopadhyay, P., Saha, S. K., Suryachandra, A. R., Raghu, M., et al. (2014b). Simulation of monsoon intraseasonal variability in NCEP CFSv2 and its role on

systematic bias. *Climate Dynamics, 43,* 2725. https://doi.org/10.1007/s00382-014-2089-5.

Griffies, S. M., Harrison, M. J., Pacanowski, P., & Rosati, A. (2004). A technical guide to MOM4, GFDL Ocean Group Tech. Rep. 5, GFDL.

Hazra, A., Chaudhari, H. S., & Dhakate, A. (2016). Evaluation of cloud properties in the NCEP CFSv2 model and its linkage with Indian summer monsoon. *Theoretical and Applied Climatology.* https://doi.org/10.1007/s00704-015-1404-3.

Hazra, A., Chaudhari, H. S., Rao, A. S., Goswami, B. N., Dhakate, A., Pokhrel, S., et al. (2015). Impact of revised cloud microphysical scheme in CFSv2 on the simulation of Indian summer monsoon. *International Journal of Climatology.* https://doi.org/10.1002/joc.4320.

Iacono, M. J., Mlawer, E. J., Clough, S. A., & Morcrette, J.-J. (2000). Impact of an improved longwave radiation model, RRTM, on the energy budget and thermodynamic properties of the NCAR Community Climate Model, CCM3. *Journal of Geophysical Research, 105,* 14873–14890.

Kanamitsu, M., Ebisuzaki, W., Woollen, J., Yang, S.-K., Hnilo, J. J., Fiorino, M., et al. (2002). NCEP-DEO AMIP-II Reanalysis (R-2). *Bulletin of the American Meteorological Society, 83,* 1631–1643.

Kang, I. S., Jin, K., Wang, B., Lau, K. M., Shukla, J., Krishnamurthy, V., et al. (2002). Intercomparision of the climatological variations of Asian Summer Monsoon precipitation simulated by 10 GCMS. *Climate Dynamics, 19,* 383–395.

Kang, I. S. & Shukla, J. (2005). Dynamical seasonal prediction and predictability of monsoon. The Asian Monsoon, edited by B. Wang, Praxis, Chichester, pp. 585–612.

Malik, A., Brönnimann, S., Stickler, A., Christoph, C. R., Stefan, M., Julien, A., et al. (2017). Decadal to multi-decadal scale variability of Indian summer monsoon rainfall in the coupled ocean-atmosphere-chemistry climate model SOCOL-MPIOM. *Climate Dynamics.* https://doi.org/10.1007/s00382-017-3529-9.

Misra, V., & Li, H. (2014). The seasonal predictability of the Asian summer monsoon in a two-tiered forecast system. *Climate Dynamics, 42*(9/10), 2491–2507.

Mlawer, E. J., Taubman, S. J., Brown, P. D., Iacono, M. J., & Clough, S. A. (1997). Radiative transfer for inhomogeneous atmospheres: RRTM, a validated correlated-k model for the longwave. *Journal of Geophysical Research, 102,* 16663–16682.

Pan, H.-L., & Mahrt, L. (1987). Interaction between soil hydrology and boundary layer developments. *Boundary-Layer Meteorology, 38,* 185–202.

Pattanaik, D. R., & Kumar, A. (2010). Prediction of summer monsoon rainfall over India using the NCEP climate forecast system. *Climate Dynamics.* https://doi.org/10.1007/s00382-009-0648-y.

Pillai, P. A., & Aher, V. R. (2016). Role of monsoon intraseasonal oscillation and its interannual variability in simulation of seasonal mean in CFSv2. *Theoretical and Applied Climatology.* https://doi.org/10.1007/s00704-016-2006-4.

Pillai, P. A., Rao, S. A., George, G., Rao, D. N., Mahapatra, S., Rajeevan, M., et al. (2017). How distinct are the two flavors of El Niño in retrospective forecasts of Climate Forecast System version 2 (CFSv2)? *Climate Dynamics, 48,* 3829–3854. https://doi.org/10.1007/s00382-016-3305-2.

Pokhrel, S., Dhakate, A., Chaudhari, H. S., & Saha, S. K. (2013). Status of NCEP CFS vis-a-vis IPCC AR4 models for the

simulation of Indian summer monsoon. *Theoretical and Applied Climatology, 111*(1–2), 65–78.

Pokhrel, S., Rahaman, H., Parekh, A., Saha, S. K., Dhakate, A., Chaudhari, H. S., et al. (2012). Evaporation-precipitation variability over Indian Ocean and its assessment in NCEP Climate Forecast System (CFSv2). *Climate Dynamics.* https://doi.org/10.1007/s00382-012-1542-6.

Pokhrel, S., Saha Subodh, K., Dhakate, A., Rahman, H., Chaudhari, H. S., Salunke, K., et al. (2016). Seasonal prediction of Indian summer monsoon rainfall in NCEP CFSv2: forecast and predictability error. *Climate Dynamics.* https://doi.org/10.1007/s00382-015-2703-1,2305-2326.

Preethi, B., Kripalani, R. H., & Kumar, K. K. (2010). Indian summer monsoon rainfall variability in global coupled ocean-atmospheric models. *Climate Dynamics, 35,* 1521–1539. https://doi.org/10.1007/s00382-009-0657-x.

Rajeevan, M., J. D. Kale, and J. Bhate, 2005. High-resolution gridded daily rainfall data for Indian monsoon studies, Tech. Rep. 2, Natl. Weather Serv., Pune, India.

Rajeevan, M., Nanjundiah, R. S. (2009). Coupled model simulations of twentieth century climate of the Indian summer monsoon. In: Mukunda N (ed) Current trends in science-platinum jubilee special. Indian Academy of Science, pp. 537–567. http://www.ias.ac.in/academy/pjubilee/book.html.

Rajeevan, M., Unnikrishnan, C. K., & Preethi, B. (2012). Evaluation of the ENSEMBLES multi-model seasonal forecasts of Indian summer monsoon variability. *Climate Dynamics, 38,* 2257–2274. https://doi.org/10.1007/s00382-011-1061-x.

Ramu, D. A., Sabeerali, C. T., Chattopadhyay, R., Rao, D. N., George, G., Dhakate, A. R., et al. (2016). Indian summer monsoon rainfall simulation and prediction skill in the CFSv2 coupled model: Impact of atmospheric horizontal resolution. *Journal of Geophysical Research, 121,* 1–17. https://doi.org/10.1002/2015jd024629.

Ratna, S. B., Sikka, D. R., Dalvi, M., & Venkata Ratnam, J. (2011). Dynamical simulation of Indian summer monsoon circulation, rainfall and its interannual variability using a high resolution atmospheric general circulation model. *International Journal of Climatology, 31*(13), 1927–1942. https://doi.org/10.1002/joc.2202.

Ratnam, J. V., Sikka, D., Kaginalkar, A., Kesarkar, A., Jyothi, N., Banerjee, S., et al. (2007). Experimental seasonal forecast of monsoon 2005 using T170L42 AGCM on PARAM Padma. *Pure and Applied Geophysics, 164,* 1641. https://doi.org/10.1007/s00024-007-0242-3.

Reynolds, R. W., Rayner, N. A., Smith, T. M., Stokes, D. C., & Wang, W. (2002). An improved in situ and satellite SST analysis for climate. *Journal of Climate, 15,* 1609–1625.

Sabeerali, C. T., Ramu, D. A., Dhakate, A., Salunke, K., Mahapatra, S., & SuryachandraRao, A. (2013). Simulation of boreal summer intraseasonal oscillations in the latest CMIP5coupled GCMs. *Journal of Geophysical Research Atmosphere*, *118*(10), 4401–4420. https://doi.org/10.1002/jgrd.50403.

Saha, Subodh K., Pokhrel, S., Salunke, K., Dhakate, A., Chaudhari, H. S., Rahaman, H., et al. (2016). Potential predictability of Indian summer monsoon rainfall in NCEP CFSv2. *Journal of Advances in Modeling Earth Systems, 8,* 1–25. https://doi.org/10.1002/2015ms000542.

Saha, S., et al. (2010). The NCEP climate forecast system reanalysis. *Bulletin of the American Meteorological Society, 91,* 1015–1057.

Sahai, A. K., Chattopadhyay, R., Susmitha, J., Mandal, R., Dey, A., Abhilash, S., et al. (2015). Real-time performance of a multi-model ensemble-based extended range forecast system in predicting the 2014 monsoon season based on NCEP-CFSv2. *Current Science, 109,* 1802. https://doi.org/10.18520/v109/i10/1802-1813.

Sahai, A. K., Sharmila, S., Abhilash, S., Chattopadhyay, R., Borah, N., Krishna, R. P. M., et al. (2013a). Simulation and extended range prediction of monsoon intraseasonal oscillations in NCEP CFS/GFS version 2 framework. *Current Science, 104,* 1394–1408.

Sahai, A. K., et al. (2013b). Special section: Atmospheric and Oceanic sciences. *Current Science, 104*(10), 1394–1408.

Seo, K.-H., Schemm, J.-K. E., Wang, W., & Kumar, A. (2007). The boreal summer intraseasonal oscillations simulated in the NCEP Climate Forecast System: The effect of Sea Surface Temperature. *Monthly Weather Review*, *135*, 1807–1827.

Shukla, R. P., & Huang, B. (2015). Mean state and interannual variability of the Indian summer monsoon simulation by NCEP CFSv2. *Climate Dynamics, 46*, 3845–3864. https://doi.org/10.1007/s00382-015-2808-6.

Sikka, D. R., & Ratna, Satyaban Bishoyi. (2011). On improving the ability of a high-resolution atmospheric general circulation model for dynamical seasonal prediction of the extreme seasons of the Indian summer monsoon. *MAUSAM, 62*(3), 339–360.

Troen, L., & Mahrt, L. (1986). A simple model of the atmospheric boundary layer: Sensitivity to surface evaporation. *Boundary-Layer Meteorology, 37,* 129–148. https://doi.org/10.1007/BF00122760.

Wang, B., Ding, Q., Fu, X., Kang, I. S., Jin, K., Shukla, J., et al. (2005). Fundamental challenge in simulation and prediction of summer monsoon rainfall. *Geophysical Research Letters, 32,* L15711.

Wang, B., Kang, I. S., & Lee, Y. J. (2004). Ensemble simulations of Asian-Australian monsoon variability during 1997/1998 El Nino by 11 AGCMs. *Journal of Climate, 17,* 803–818.

Winton, M. (2000). A reformulated three-layer sea ice model. *Journal of Atmospheric and Oceanic Technology., 17,* 525–531.

Wu, X., Simmonds, I., & Budd, W. F. (1997). Modeling of Antarctic sea ice in a general circulation model. *Journal of Climate, 10,* 593–609.

Yang, S., Zhang, Z., Kousky, V. E., Higgins, R. W., Yoo, S.-H., Liang, J., et al. (2008). Simulations and seasonal prediction of the Asian summer monsoon in the NCEP climate forecast system. *Journal of Climate, 21,* 3755–3775. https://doi.org/10.1175/2008JCLI1961.1.

Zheng, Y., Shinoda, T., Lin, J.-L., & Kiladis, G. N. (2011). Sea surface temperature biases under the stratus cloud deck in the southeast pacific ocean in 19 IPCC AR4 coupled general circulation models. *Journal of Climate*, *24*(15), 4139–4164.